Frascati Physics Series Vol. nnn (2001), pp. 000-000
Heavy Quarks at Fixed Target - Rio de Janeiro, Oct. 9-19, 2000

Rare K^+ Decays from Experiment E787

Vivek Jain
Brookhaven National Laboratory

ABSTRACT

This paper presents the latest results from experiment E787, at Brookhaven National Laboratory, on $K^+ \to \pi^+ \nu\overline{\nu}$ and radiative K^+ decays. The result for $K^+ \to \pi^+ \nu\overline{\nu}$ uses data collected in runs taken during 1995, 1996 and 1997. In addition, we discuss plans for future measurements of $K^+ \to \pi^+ \nu\overline{\nu}$.

1 Theoretical Background

1.1 $K^+ \to \pi^+ \nu\overline{\nu}$

This decay mode is a very clean probe of the dynamics of the Cabbibo-Kobayashi-Maskawa (CKM) mixing matrix. It is a $\Delta S = 1$ process which proceeds via the box diagram and electroweak penguin diagrams [1)]. Since the top quark is so much more massive than the other up-type quarks, its contribution dominates

the decay rate. In addition, long distance effects are small and the hadronic matrix element can be obtained from the semi-leptonic decay $K^+ \to \pi^0 e^+ \nu_e$ (K_{e3}). As a result, the theoretical uncertainty in understanding the decay rate is rather low (theoretical error is $\approx 7\%$, most of it is due to the charm quark contribution). The rate can be expressed (in the Standard Model) as,

$$B(K^+ \to \pi^+ \nu\overline{\nu}) = \frac{\kappa_+ \alpha^2 B(K_{e3})}{2\pi^2 \sin^4 \theta_W |V_{us}|^2} \Sigma_l |X_t \lambda_t + X_c^l \lambda_c|^2 \qquad (1)$$

where, κ_+ is the isospin correction, $\lambda_t = V_{ts} V_{td}^*$, $\lambda_c = V_{cs} V_{cd}^*$, and $X_{t(c)}$ are Inami-Lim functions [1], and the sum Σ_l is over the three neutrino flavours. Using measurements from the K and B systems, to determine parameters of the CKM matrix, which are used as inputs, one can predict,

$$0.5 \times 10^{-10} < \ \mathrm{B}(K^+ \to \pi^+ \nu\overline{\nu}\ ) \ < 1.2 \times 10^{-10}$$

This range is due to the uncertainties in the input parameters. Since the top quark dominates the proceedings, this decay mode provides a very clean measurement of V_{td}. This measurement is complementary to the measurement of V_{td} from $B_d^0 \overline{B}_d^0$ mixing. A difference in the value of V_{td} extracted from these two sources, could suggest new physics, since any new phenomena would, in general, affect the K and B systems differently.

1.2 Radiative K^+ decays

Radiative K^+ decays come from two sources, (a) the "pedestrian" Inner Bremsstrahlung decay, where a charged decay daughter emits a photon, and (b) the more interesting structure dependent (SD) part. In this paper, we are concerned with the SD contribution.

The latter source is a good testing ground for Chiral Perturbation theory (χPT), and is also important for measuring long distance contributions to other decays of interest, *e.g.*, $K_L^0 \ \to \ l^+ l^- \gamma\gamma$ is a background to $K_L^0 \ \to \ \pi^0 l^+ l^-$.

For $K^+ \to \mu^+ \nu_\mu \gamma$, form factors for the SD part, $\mathrm{F_A}$ and $\mathrm{F_V}$ are predicted by χPT. $K^+ \to \pi^+ \pi^0 \gamma$ is interesting in its own right; decay rates for K^+, K_L and K_S could be similar, even though the decay rates for the non-photonic final state ($\pi\pi$) are very dissimilar, also, some SUSY models predict that K^+ and K^- decay rates are unequal, leading to direct CP violation.

2 Search for $K^+ \to \pi^+ \nu\overline{\nu}$

2.1 Experimental Design

Since the expected branching fraction is $\approx 10^{-10}$, backgrounds are **the** major concern, consequently, the entire experiment and the analysis techniques are geared towards reducing backgrounds while maintaining a reasonable detection efficiency.

The two major backgrounds are $K^+ \to \mu^+\nu$ (BR=64%) and $K^+ \to \pi^+\pi^0$ (BR=21%). Other sources, *e.g.*, $K^+ \to \pi^0 e^+ \nu_e$, $K^+ \to \pi^0 \mu^+ \nu_\mu$, etc., are not as daunting. Fig. 1 shows the momentum spectrum of charged tracks in major K^+ decays. The experimental strategy is set by the characteristics of the backgrounds.

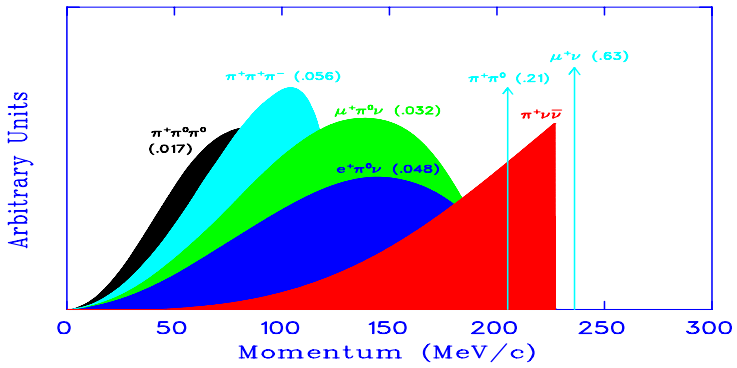

Figure 1: *Momentum spectrum of charged tracks produced in K^+ decays*

Since the two largest decay modes give off mono-energetic charged daughters (P_π = 205 MeV/c and P_μ = 236 MeV/c, respectively), we stop the incident beam and let the K^+ decay at rest. If we maintain very good kinematic resolution, and search in a momentum region inside this range, we have one discriminant against these two background sources (the momentum spectrum in Fig. 1 for the π^+ in $K^+ \to \pi^+ \nu\overline{\nu}$ decays has been enhanced by $\sim 10^{10}$). We also use the energy and range of the tracks as part of the kinematic discriminant.

To further discriminate against muons, we detect the decay chain, $\pi^+ \to \mu^+ \to e^+$. To do this, we require that the outgoing π^+/μ^+ stop in the

detector and decay. The π^+ will generate a μ^+ and an e^+, whereas a muon will only give rise to an e^+.

Most K^+ decays produce a π^0 in the final state, so we designed the experiment to have very good photon veto capabilities, e.g., the average rejection for the π^0 in $K^+ \to \pi^+\pi^0$ is about 10^6.

There are other sources, *e.g.* pions in the incident beam which scatter in the target and fall inside the signal region, charge exchange where a K^+ turns into a K_L, and the latter decays semi-leptonically. Such sources can be cut out by requiring that the outgoing pion be detected a few nano-seconds after the incident K^+ enters the target. This not only drastically reduces the possibility that an incoming pion scatters into the fiducial region, but also ensures that the incoming K^+ decays at rest.

The E787 has been described in detail elsewhere [2]. Its main features are a *degrader* to slow the incident K^+'s, so that they come to rest in an *active target* which is mainly composed of 413 5mm scintillating fibers. The target is surrounded by a *drift chamber*, and a *range stack* composed of 21 layers of plastic scintillators. The outgoing daughter pions are required to stop in the range stack, where we detect the $\pi \to \mu \to e$ decay chain using *500 MHz transient digitizers*. Photons are detected with an extensive system of *photon veto detectors*, e.g., Pb-Scintillator calorimeter in the central region, CsI crystals in the endcap regions, etc. Track momentum is measured in the presence of a 1T solenoidal magnetic field.

2.2 "Online" improvements

Since we first published the observation of this decay mode [3] using data collected in 1995, we have taken more data during runs in 1996, 1997 and 1998. We have made many improvements; lowering the momentum of the K^+ beam, which results in a higher fraction of incident K^+ stopping in the target and a reduction in background hits from K^+ interactions in the degrader, improvements to the trigger, increased acceptance for detecting $\mu \to e$ decays, etc.

In Table 1, we present some details of the data runs in 1995-97.

Even though the data runs were shorter in 1996 and 1997, we still collected more data as compared to the run in 1995. This was entirely due to the improvements outlined above.

Table 1: *1995-97 dataset*

	1995	1996	1997	Total
Length of run (weeks)	25	17	8	
Triggers (10^{12})	~ 1.53	~ 1.16	~ 0.59	~ 3.28
No. of evts. to tape				$\sim 3.1 \times 10^8$

3 Offline Analysis

Since the backgrounds are orders of magnitude larger than the signal, the analysis has to be designed very carefully. Some of the main features are,

(a) *Blind Analysis* The signal region is hidden (by inverting cuts) while cuts are developed and background levels are estimated. To avoid any bias in the background estimates, we develop cuts on 1/3 of the dataset and take the (actual) background level from the remaining 2/3 of the data and extrapolate the latter to the full sensitivity.

(b) *"Bifurcated" Analysis* In the analysis, we make an *"a priori"* identification of the background sources and then develop at least two independent cuts for each source. In this manner, we can measure the rejection of each cut using the data itself. For instance, $K^+ \to \pi^+\pi^0$ is rejected using kinematic cuts based on measuring the Range, Momentum and Energy of the outgoing π^+ AND photon veto cuts which work on detecting the π^0. Similarly, $K^+ \to \mu^+\nu_\mu$ is rejected by applying kinematic cuts on the μ and by requiring the presence of the $\pi^+ \to \mu^+ \to e^+$ decay chain.

The goals for the analysis of the 1996-97 datasets and the re-analysis of the 1995 dataset were (a) to increase rejection so as to keep the total background at the same level as in the original result [3], (b) maintain or (possibly) increase detection efficiency, and (c) devise methods to increase background samples which would lead to a better understanding and a more precise estimation of the background.

A lot of improvements were made in the analysis; tracking changes in the target, range stack and drift chamber improved the resolution in range and momentum, a better electron (from μ decay) finding algorithm was put in place, new cuts were devised to reject K^+ decays in flight, etc. For instance, the new analysis had a 30% larger rejection (with the same acceptance) against muon backgrounds.

The background estimates for the 1995-97 dataset are presented in Table2.

Table 2: *Background Estimate for 1995-97 datasets*

	Total
$K^+ \to \pi^+\pi^0$	0.020 ± 0.01
$K^+ \to \mu^+\nu_\mu$	0.030 ± 0.01
1(&2)-beam	0.020 ± 0.02
Charge Exchange	0.010 ± 0.01
Total	0.08 ± 0.02

The background estimate in the published result [3] was 0.08 ± 0.03, which implies that we increased rejection by a factor of about 2.2. At the same time, we were able to increase acceptance from 0.16% to 0.21% (an increase of almost 30%).

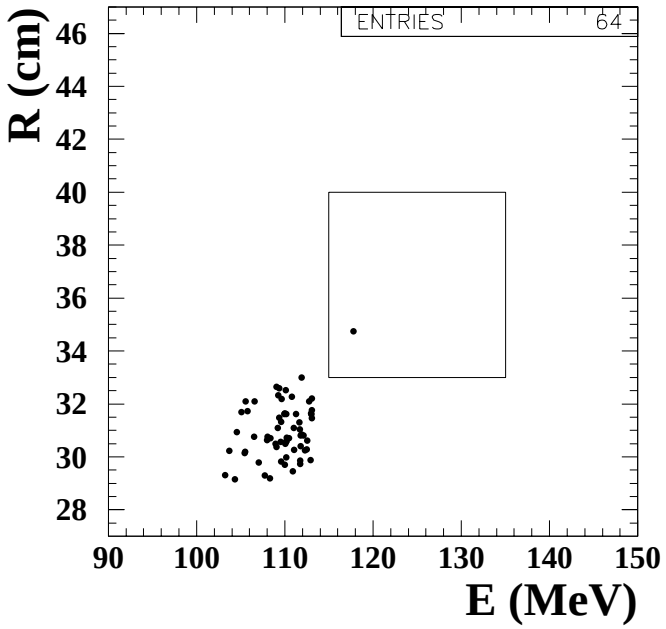

Figure 2: *Result for 1995-97 datasets*

In Fig.2, we present the results from the 1995-97 datasets. The plot shows the data after all cuts, except those on Energy and Range of the π^+, have been

made. We have one event in the signal region. Using the total luminosity and detection efficiency, we obtain [4)]

$$\mathcal{B}(K^+ \to \pi^+ \nu\overline{\nu}) = 1.5^{+3.4}_{-1.2} \times 10^{-10} \tag{2}$$

Assuming unitarity of the CKM matrix and V_{cb}, this result implies, $0.002 \leq |V_{td}| \leq 0.04$.

4 Results on Radiative Decays

4.1 $K^+ \to \pi^+\pi^0\gamma$

We have 19,836 events in this decay channel [5)], which represents an increase of a factor of eight in statistics over the previous best measurement.

The data is expressed in terms of a variable W, which is defined as,

$$\begin{aligned} \mathrm{W}^2 &\equiv (\mathrm{p}\cdot\mathrm{q})/\mathrm{m}^2_{\mathrm{K}^+} \times (\mathrm{p}_+\cdot\mathrm{q})/\mathrm{m}^2_{\pi^+} \\ &= \mathrm{E}^2_\gamma \times (\mathrm{E}_{\pi^+} - \mathrm{P}_{\pi^+} \times \cos\theta_{\pi^+\,\gamma})/(\mathrm{m}^2_{\mathrm{K}^+} \times \mathrm{m}^2_{\pi^+}) \end{aligned} \tag{3}$$

where, p, p_+ and q are 4-momenta for the K^+, π^+ and gamma, respectively. The structure dependent (DE) contribution is mainly at high values of W, as shown in Fig. 3. Low values of W are populated by Inner Bremsstrahlung (IB) decays.

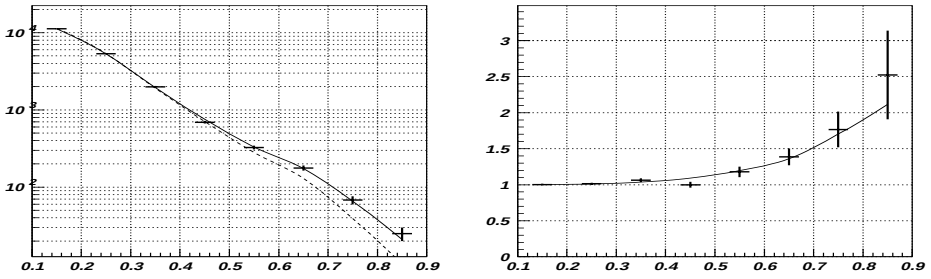

Figure 3: *(left) W spectrum of the signal events and best fits to IB+DE [solid curve] and IB alone [dashed curve]; (right) W spectrum normalized to the IB spectrum.*

We measure,

$$\mathrm{BR}(\mathrm{K}^+ \to \pi^+\pi^0\gamma; \mathrm{DE}) = (4.72 \pm 0.77) \times 10^{-6}\,(55 < \mathrm{T}_{\pi^+} < 90\mathrm{MeV}) \tag{4}$$

This result is roughly a factor of 4 lower than previous measurements. In addition, the interference, between IB and DE, is measured to be $(-0.4 \pm 1.6)\%$, and the ratio, DE/IB is measured to be $(1.85 \pm 0.30)\%$.

The decay rate, corrected to full phase space[1], is now measured to be similar to that for K_L: $\Gamma(K^+ \to \pi^+\pi^0\gamma; DE) = (808 \pm 132)s^{-1}$ vs. $\Gamma(K_L^0 \to \pi^+\pi^-\gamma; DE) = (617 \pm 18)s^{-1}$.

4.2 $K^+ \to \mu^+\nu_\mu\gamma$

The structure dependent (SD) contribution has two components, due to the two polarizations of the outgoing photon. SD^+ peaks at higher E_μ and E_γ and is easier to detect. We have roughly 2700 events [6] in the region of interest, $E_\gamma \geq 90MeV$ and $E_\mu \geq 137MeV$.

In Figure 4, we present the data in terms of the angle between the μ^+ and the γ. It is clear from the fits that there is a large contribution from SD.

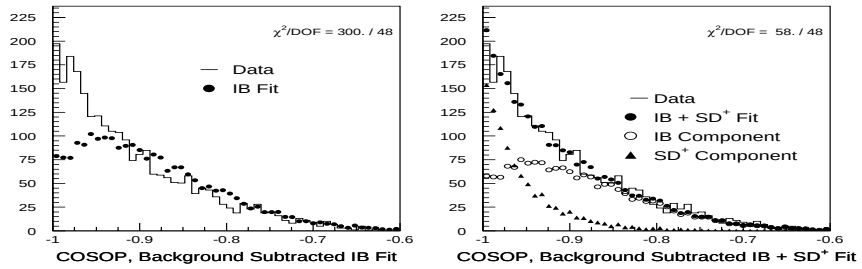

Figure 4: *Distribution of* $\cos\theta_{\mu\gamma}$ *for E787* $K^+ \to \mu^+\nu_\mu\gamma$ *candidates. A fit to IB alone is shown in (a), and a fit to both IB and* SD^+ *is shown in (b).*

The final result is based on a fit which includes contributions from SD^-, IB and interference terms,

$$B(SD^+) = (1.33 \pm 0.12 \pm 0.18) \times 10^{-5} \tag{5}$$

The sum of form factors is measured to be, $|F_V + F_A| = 0.165 \pm 0.007 \pm 0.011$. This can be compared to the $O(p^4)$ χPT calculation [7] of $F_V + F_A = 0.137 \pm 0.006$ and B(SD^+)=9.22×10^{-6}. We also measure $-0.04 \leq F_V - F_A < 0.24$ at 90% CL; this is to compared with an expectation [7] of (0.052 ± 0.006).

[1]This correction assumes that the form factor has no energy dependence.

5 Future Plans

5.1 1998 dataset

As mentioned in Section 2.2, we also took data in 1998. The sensitivity of this data set is expected to be approximately the same as that of the combined 1995-97 datasets. This result is expected in 2001.

5.2 Phase Space below $K_{\pi 2}$ peak

In the analysis presented here, we have searched for the signal in the region above the $K_{\pi 2}$ and below the $K_{\mu 2}$ momentum peaks. However, because of the V-A nature of the the decay, there is also a large phase space below the $K_{\pi 2}$ peak, as shown in Fig.1. Some of the advantages of looking in this region are, phase space is larger than above $K_{\pi 2}$, less π^+ absorption losses, etc., leading to a possibility of $\times 3$ increase in acceptance.

However, the background due to $K_{\pi 2}$ is very large, since the π^+ can elastically scatter in a fiber hit by the incoming K^+, lose energy and fall inside the signal region. Since this is a real pion, we cannot use the kinematic discriminant to reject this background. This scenario occurs when the daughter pions travel along the beam axis. Since photon veto capability is weak in this angular region, it is more likely to miss the two decay photons. One has to look for evidence of the pion scatter in the kaon fiber, as a way to discriminate against this background.

We made good progress in studying this region using the 1996 dataset. Searching in the momentum region, 140 MeV/c $\leq \mathrm{P}_\pi \leq$ 190 MeV/c, preliminary studies showed that $\mathrm{S_{SM}}$/B was $\sim$ 1:5, where $\mathrm{S_{SM}}$ is the expected Standard Model signal. We expect this ratio to improve to $\sim$ 1:3 when we extrapolate to 1995-98 datasets, and to $\sim$ 1:1 in experiment E949.

5.3 Experiment E949

Experiment E949 is an upgrade of E787 and is scheduled to run in 2002-2003, with an engineering run scheduled for 2001.

Many subsystems in E787 have been upgraded, e.g., *Photon veto* has been improved by adding more detectors in the central region, converting the current degrader into an active degrader, adding a photon veto detector downstream of the target,etc., the *Range Stack* has been improved by replacing some of the

scintillator layers, *Trigger* and *DAQ* systems have been upgraded, etc. These improvements are expected to increase sensitivity by about a factor of 3 (over the result based on the 1995 dataset [3]).

In addition, the accelerator is scheduled to deliver more protons per spill, increase the duty cycle and reduce the K^+ momentum, leading to an improvement of a factor of 2.2 in sensitivity.

We plan to reoptimize our analysis for these higher rates and also hope to gain sensitivity from looking in the phase space below the $K_{\pi 2}$ peak, as described in Section 5.2. Each of these two sources is expected to yield an increase in sensitivity of a factor of 2. However, we take a conservative approach and take only one factor of 2 in our projections.

Factoring in the increase in running time ($\sim$ 6000 hours), we estimate that our sensitivity will be a factor of 50 higher than the result based on the 1995 dataset [3], which implies a Single Event Sensitivity (SES) of about 8×10^{-12}. This means that we expect to observe 10 Standard Model events in E949, allowing us to measure V_{td} with a precision of about 23%, which is extremely competitive with the current precision of about 21% obtained from $B^0_d \overline{B}^0_d$ mixing.

6 Conclusions

Using data collected in 1995-97, we have measured ,

$$\mathcal{B}(K^+ \to \pi^+ \nu\overline{\nu}) = 1.5^{+3.4}_{-1.2} \times 10^{-10} \tag{6}$$

We have also made high statistics measurements of the structure dependent parts of $K^+ \to \pi^+\pi^0\gamma$ and $K^+ \to \mu^+\nu_\mu\gamma$.

Using all the data collected with the E787 detector, we expect to improve the SES for $K^+ \to \pi^+\nu\overline{\nu}$ to $\sim 0.7 \times 10^{-10}$.

Using the data which we expect to collect in experiment E949, we hope to observe $\mathcal{O}(10)$ $K^+ \to \pi^+\nu\overline{\nu}$ Standard Model events. This will allow us to measure V_{td} with a precision of about 23%.

In Fig.5, we present the improvement in SES. We also show the expectations from the 1995-98 datasets (denoted as E787 final), from experiment E949, and from a proposed experiment (CKM) at Fermilab [8].

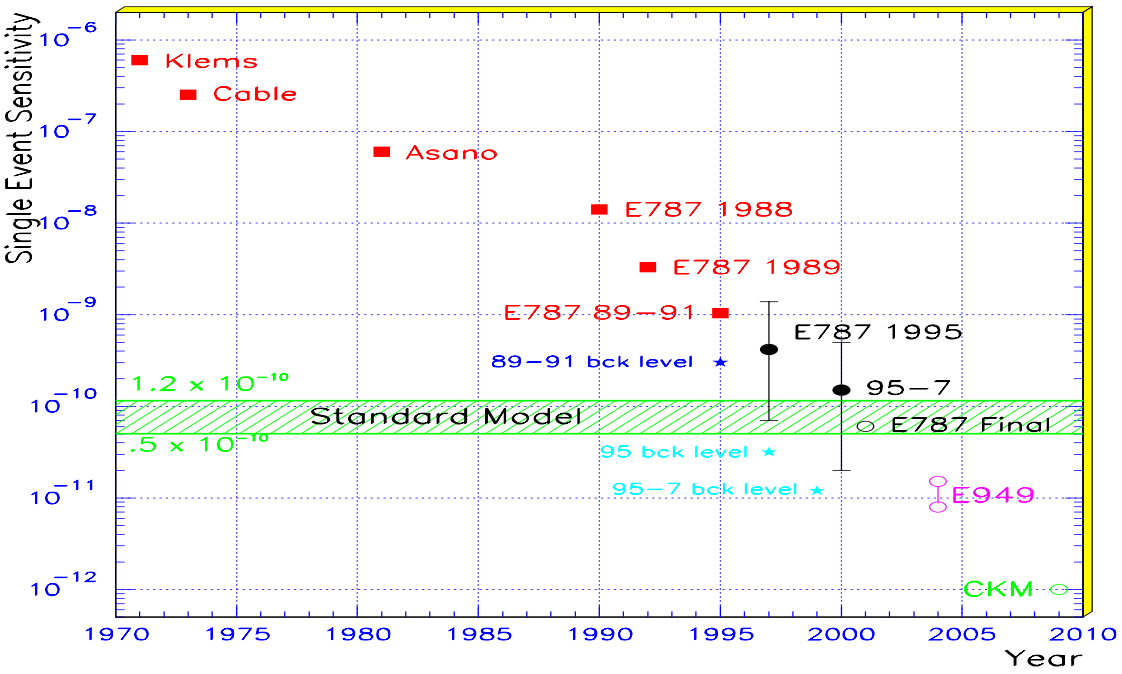

Figure 5: *Single Event Sensitivity*

References

1. A. Buras and R. Fleischer, Los Alamos e-archive, hep-ph/9704376
2. T.K. Komatsubara *et. al.,* Nucl. Instrum. Methods Phys. Res., Sect A **404**, 315 (1198) and references within
3. S. Adler *et. al.,* Phys. Rev. Lett. **79**, 2204 (1997)
4. S. Adler *et. al.,* Phys. Rev. Lett. **84**, 3768 (2000)
5. S. Adler *et.al* Phys. Rev. Lett. **85**, 4856 (2000)
6. S. Adler *et. al.* Phys. Rev. Lett. **85**, 2256 (2000)
7. J. Bijnens *et al.*, Nucl.Phys. **B396**, 81 (1993)
8. See talk by Hogan Nguyen at this conference